

# Journal of Materials Chemistry C

Materials for optical, magnetic and electronic devices

[rsc.li/materials-c](https://rsc.li/materials-c)



ISSN 2050-7526

**PAPER**

Francisco Rivadulla *et al.*  
Light-induced bi-directional switching of thermal  
conductivity in azobenzene-doped liquid crystal  
mesophases

Cite this: *J. Mater. Chem. C*, 2023, 11, 4588

## Light-induced bi-directional switching of thermal conductivity in azobenzene-doped liquid crystal mesophases†

Noa Varela-Domínguez,<sup>a</sup> Carlos López-Bueno,<sup>a</sup> Alejandro López-Moreno,<sup>‡,b</sup> Marcel S. Claro,<sup>a</sup> Gustavo Rama,<sup>b</sup> Víctor Leborán,<sup>c</sup> María del Carmen Giménez-López<sup>b</sup> and Francisco Rivadulla<sup>b,\*</sup>

The development of systems that can be switched between states with different thermal conductivities is one of the current challenges in materials science. Despite their enormous diversity and chemical richness, molecular materials have been only scarcely explored in this regard. Here, we report a reversible, light-triggered thermal conductivity switching of  $\approx 30\text{--}40\%$  in mesophases of pure 4,4'-dialkyloxy-3-methylazobenzene. By doping a liquid crystal matrix with the azobenzene molecules, reversible and bidirectional switching of the thermal conductivity can be achieved by UV/Vis-light irradiation. Given the enormous variety of photoactive molecules and chemically compatible liquid crystal mesophases, this approach opens unforeseen possibilities for developing effective thermal switches based on molecular materials.

Received 9th January 2023,  
Accepted 23rd February 2023

DOI: 10.1039/d3tc00099k

rsc.li/materials-c

## Introduction

Controlling the thermal conductivity of a material using an external stimulus could change the way we deal with the problem of thermal dissipation in microelectronics or the efforts to increase the efficiency of thermoelectric energy conversion devices. During the last few years, this research focused mostly on solid-state devices, particularly ferroelectrics: ferroelectric/ferroelastic domain walls are effective phonon scatterers, whose density can be regulated by an electric field and/or strain.<sup>1–3</sup>

In a soft-matter side approach to the problem, Ishibe *et al.*<sup>4</sup> showed that block copolymers may be engineered to show a reversible change in their thermal conductivity, although in this case is linked to the transition temperature between different types of ordering. Tomko *et al.*<sup>5</sup> achieved a large and

reversible switching of the thermal conductivity of bio-polymer networks upon hydration/dehydration cycles.

On the other hand, Shin *et al.*<sup>6</sup> use UV/Vis irradiation cycles to tune the thermal conductivity of photoresponsive polymers. Light modulates the  $\pi\text{--}\pi$  interactions among the polymer aromatic rings and triggers an actual crystal-to-liquid transition, resulting in a  $\sim 60\%$  change in the thermal conductivity.<sup>7</sup> This is a very controllable approach, which allows remote control of the thermal conductivity of the system, and whose only drawback is, perhaps, the lack of full reversibility of the liquid crystal (LC)-to-isotropic liquid (IL) in some photo-responsive polymers, which is sometimes compromised due to the lack of orientational mobility of the *trans* isomers at room temperature.<sup>8</sup>

This could be overcome by synthesizing azobenzene derivatives that self-assemble into 3D crystals or liquid crystals (LC) mesophases at or close to room temperature;<sup>9</sup> these form photo-active mesophases whose thermal transport could be directly modified by UV/Vis irradiation.

Here we report large (up to 40%) reversible switching of the thermal conductivity of photochromic 4,4'-dialkyloxy-3-methylazobenzene derivatives by isothermal UV/Vis illumination at room temperature.

More important, we demonstrate that photoactive 4,4'-dialkyloxy-3-methylazobenzene molecules can be doped into achiral LC matrixes to induce a complete and reversible molecular reorganization of the mesophase under UV/Vis irradiation and therefore a large change in the thermal conductivity of the whole system. Depending on the molecular arrangement of the host mesophase,

<sup>a</sup> CiQUS, Centro Singular de Investigación en Química Biolóxica e Materiais Moleculares, Departamento de Química-Física, Universidade de Santiago de Compostela, 15782-Santiago de Compostela, Spain. E-mail: f.rivadulla@usc.es

<sup>b</sup> CiQUS, Centro Singular de Investigación en Química Biolóxica e Materiais Moleculares, Departamento de Química-Inorgánica, Universidade de Santiago de Compostela, 15782-Santiago de Compostela, Spain

<sup>c</sup> CiQUS, Centro Singular de Investigación en Química Biolóxica e Materiais Moleculares, Universidade de Santiago de Compostela, 15782-Santiago de Compostela, Spain

† Electronic supplementary information (ESI) available: Details of the synthesis, UV-Vis absorption spectra of the azobenzene films, DSC and POM scans, and NMR spectra of all the molecules synthesized for this work. See DOI: <https://doi.org/10.1039/d3tc00099k>

\* Present address: IMDEA Nanociencia, C/ Faraday 9, Madrid, Spain.



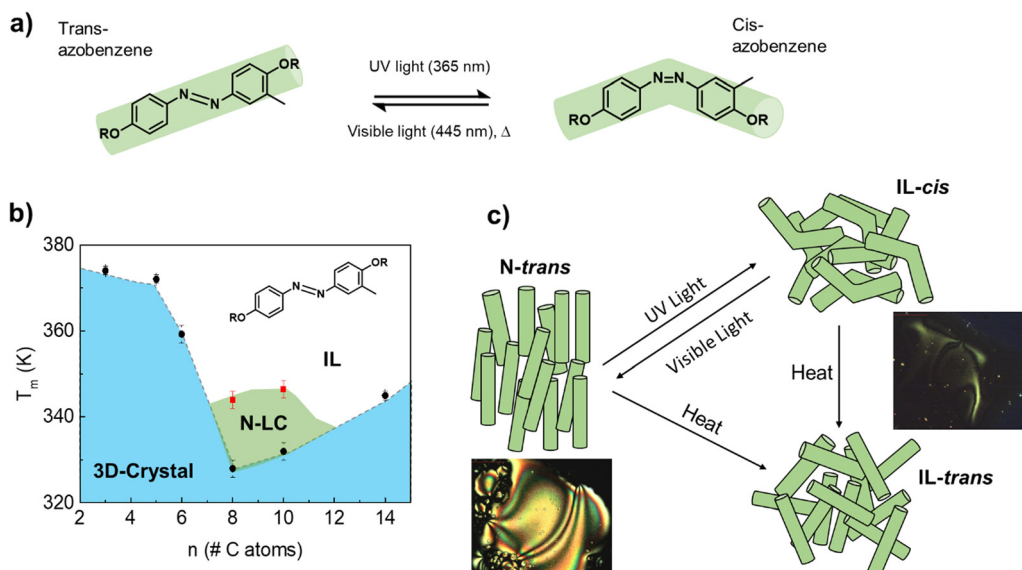


**Fig. 1** (a) Scheme of the light-induced isomerization between the rod-*trans* and the bended-*cis* molecular structures of the azobenzene derivatives studied in this work. (b) Phase diagram of the 4,4'-dialkyloxy-3-methylazobenzene derivatives with the number of C-atoms in the alkyl chain; N-LC and IL refer to nematic liquid crystal and isotropic liquid, respectively. The transition temperatures that mark the stability limits of each phase were obtained from DSC experiments (see Fig. 2 and the ESI†). (c) Scheme of the different phases, related to the two molecular isomers, achievable with temperature and UV/Vis light irradiation. The images were taken on a polarized optical microscope (POM); see Fig. S2–S4 (ESI†).

either a reversible increase or decrease of the thermal conductivity may be achieved upon UV/Vis illumination (bi-directional switching). The use of photoactive molecular machines<sup>10</sup> showing a light-dependent photoresponse to control the thermal conductivity of LC opens a new path for the design of molecular bi-directional thermal switches.

## Results and discussion

Azobenzene-based molecules undergo reversible isomerization between the thermodynamically stable, rod-like *trans* configuration and the bent *cis* molecular structure, when irradiated with UV/visible light (Fig. 1a). Norikane *et al.*<sup>11,12</sup> showed that inserting a methyl group at the *meta*-position of one of the benzene rings, breaks the molecular symmetry of dialkyloxy-chain azobenzenes, and drastically reduces the energy for the photoinduced crystal-to-liquid phase transition. For instance, a reversible transformation into a viscous IL was demonstrated by Norikane *et al.*<sup>11</sup> in 4,4'-dialkyloxy-3-methylazobenzene derivatives with 6, 10, and 12 carbon atoms in the alkyl chain, after irradiating the samples at room temperature with 365 nm light ( $\approx 100 \text{ mW cm}^{-2}$ ). However, no transition was observed in the totally symmetric structures, either the 4,4'-dialkyloxy-azobenzene or the 4,4'-dialkyloxy-3,6-dimethylazobenzene, under the same conditions.

Therefore, this family of asymmetric molecules could provide a good starting point in the search for photochromic molecular materials where reversible thermal conductivity states can be achieved under mild conditions. To prove this hypothesis, we synthesized a series of 4,4'-dialkyloxy-3-methylazobenzene rod-like derivatives with  $-\text{OR} = -\text{OC}_n\text{H}_{2n+1}$   $n = 3, 5, 6, 8, 10, \text{ and } 14$

(Fig. 1b; see the ESI† for details of the synthesis). NMR spectroscopy confirmed that the *trans* isomer is the thermodynamically stable phase for all the alkyl chain lengths (only  $\approx 10\%$  of the *cis* isomers remain in the  $n = 5$  phase at room temperature; see NMR data in the supporting information). The limits of thermal stability of the crystalline and N-LC phases were studied by differential scanning calorimetry (DSC) and polarized optical microscopy (POM); see Fig. S2–S4, ESI†). Increasing the length of the alkyl chain in the rod-like molecule induces preferential alignment along one spatial direction, destabilizing the 3D-crystal in favor of a Nematic LC (N-LC).

DSC measurements and thermal conductivity,  $\kappa(T)$ , curves are shown in Fig. 2 for the  $n = 6, 8, \text{ and } 10$  azobenzene derivatives. The  $n = 6$  system transits directly from a 3D crystal to an IL at  $\approx 358 \text{ K}$ , while for the  $n = 8$  and  $n = 10$ , there is an intermediate N-LC between the 3D crystal and the IL.

The  $\kappa(T)$  of the azobenzene derivatives was monitored continuously in a cryostat during heating/cooling cycles at  $1 \text{ K min}^{-1}$  (see the ESI† and ref. 13 for further details of our experimental setup and the  $3\omega$  method used to measure  $\kappa$ ).

As shown in Fig. 2,  $\kappa(T)$  shows an excellent sensitivity to the molecular rearrangements occurring during thermal cycling.

The value of  $\kappa$  in the 3D crystal is quite low,  $\approx 0.2\text{--}0.3 \text{ W m}^{-1} \text{ K}^{-1}$ , similar to amorphous polymers and molecular liquids,<sup>14</sup> and it is only slightly larger than in the *trans*-IL occurring at high temperature, despite the lack of translational symmetry in the latter. The lower  $\kappa$  in the N-LC than in the IL confirms the planar alignment of the mesophase.<sup>15,16</sup>

In Fig. 3 we show the effect of UV/Vis illumination on  $\kappa$  for  $n = 10$  (similar qualitative behavior was observed in the other systems studied in this work). Irradiation of the film with UV light (365 nm,  $\approx 160 \text{ mW cm}^{-2}$ ) at room temperature



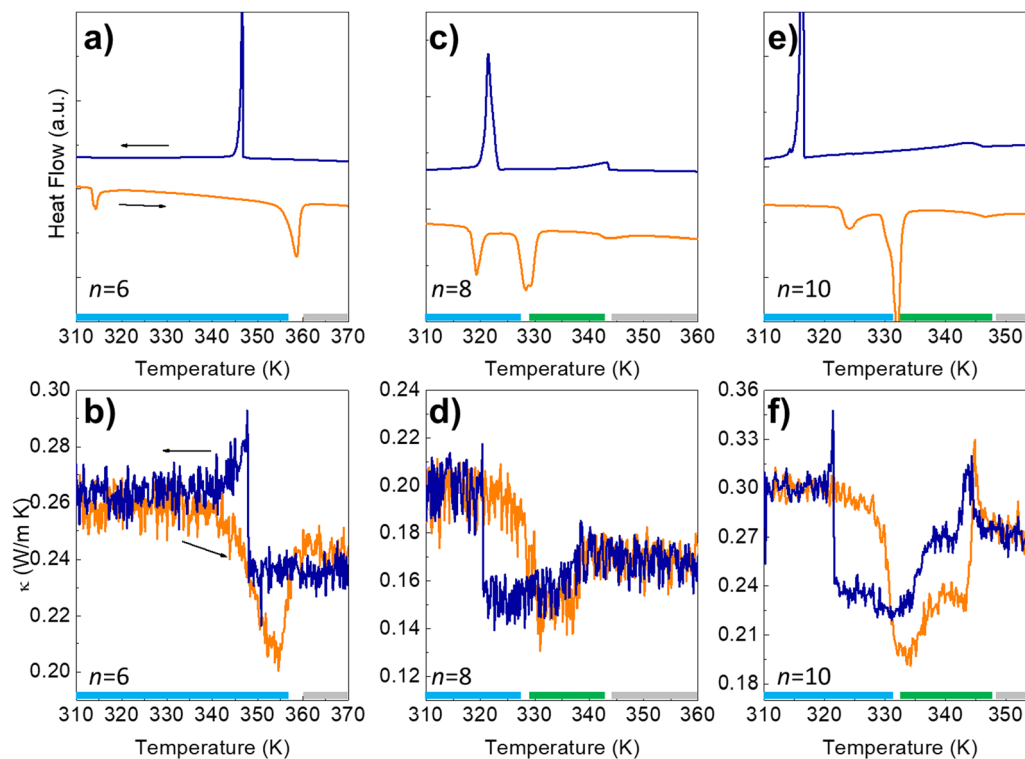


**Fig. 2** (a, c and e) Differential Scanning Calorimetry (DSC) and thermal conductivity (b, d and f) for the 4,4'-dialkoxy-3-methylazobenzene with  $n = 6$ , 8, and 10 carbon atoms in the alkyl chains. The sharp peaks at the lower temperature on the DSC heating runs correspond to a transition between two different 3D crystal structures, while the second one marks the transition between a 3D crystal and IL ( $n = 6$ ) or between a 3D crystal and a N-LC ( $n = 8$  and 10).<sup>11</sup> The broader peak at  $\approx 343$ – $347$  K in  $n = 8, 10$  marks the stability limit of this mesophase before melting into an IL. These transitions are perfectly visible in the thermal conductivity experiments (b, d and f). The temperature range of stability of the different phases is indicated by the color bars at the bottom of each panel (blue, green, and grey for the 3D crystal, N-LC and IL, respectively); see also the phase diagram of Fig. 1b).

transforms the crystal into *cis*-IL (see also Fig. S1, ESI<sup>†</sup>), with a reduction of the  $\kappa$  of  $\approx 30$ – $40\%$ . Once UV irradiation stops, this phase change remains stable for hours in the dark, before recovering to the original phase after thermal relaxation of the

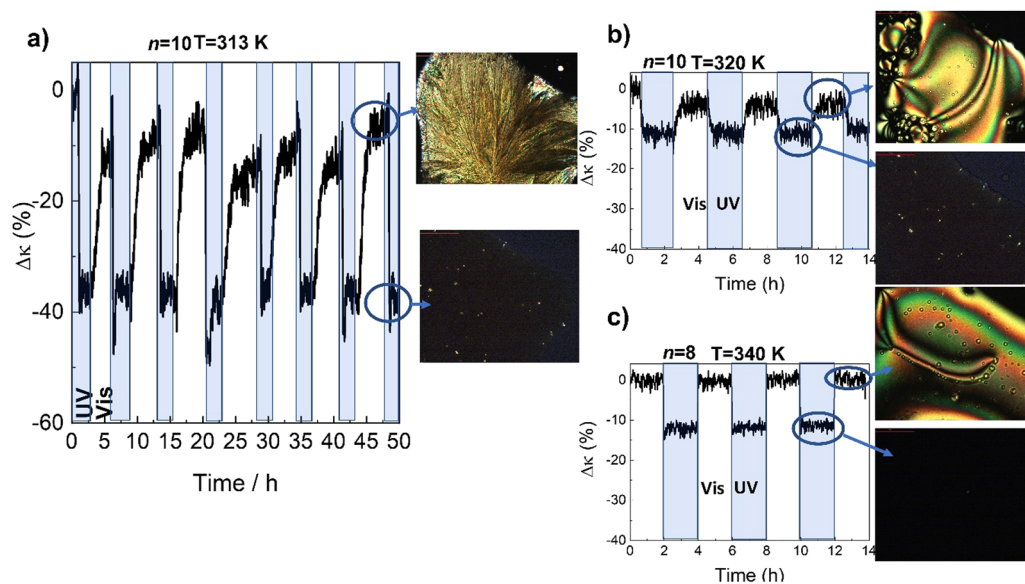


**Fig. 3** (a) Relative variation of  $\kappa$  in  $n = 10$  at 313 K under UV/Vis illumination. The transition corresponds to the isothermal 3D crystal-to-IL transformation, as shown in the POM images on the right. Relative variation of  $\kappa$  in  $n = 10$  at 320 K (b), and  $n = 8$  at 340 K (c), under UV/Vis illumination. At these temperatures, light drives the transition between the N-LC and the IL, as shown in the POM images at the right. Note the smaller thermal contrast compared to the 3D crystal to IL shown in panel (a).



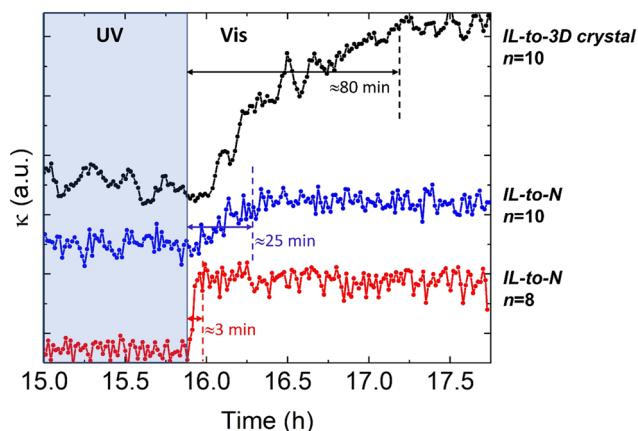


Fig. 4 Time-dependence of thermal conductivity during recovery of the ordered *trans*-phase, with visible light illumination of the isotropic-liquid in the *cis*-configuration. The figure shows the traces for the IL-to-3D crystal in  $n = 10$ , and the IL-to-N in the  $n = 10$  and  $n = 8$  (the same samples shown in Fig. 3). The curves have been displaced vertically for clarity. The recovery of the thermal conductivity is completed in 3 min for the IL-to-N of  $n = 8$ . The temperature of each experiment, as in Fig. 3, is 313 K (IL-to-3D crystal,  $n = 10$ ), 320 K (IL-to-N,  $n = 10$ ) and 340 K (IL-to-N,  $n = 8$ ), respectively.

*cis* azobenzene isomer. The recovery of the thermal conductivity can be accelerated by irradiating the IL with visible light (445 nm,  $\approx 150 \text{ mW cm}^{-2}$ ). As shown in Fig. 3a), this process can be repeated many times, demonstrating its reversibility.

Note that the observed reduction of  $\approx 30\text{--}40\%$  upon illumination means that  $\kappa$  in the *cis*-IL ( $\approx 0.2 \text{ W m}^{-1} \text{ K}^{-1}$ ) is considerably smaller than in the *trans*-IL ( $\approx 0.27 \text{ W m}^{-1} \text{ K}^{-1}$ ). We have measured a decrease of  $\approx 2\%$  in the density of the *cis*-IL compared to *trans*-IL, which seems too small to account for such a large change in  $\kappa$  ( $\approx 15\text{--}20\%$ ). Thus, this observation suggests a much less effective intermolecular (most likely  $\pi\text{--}\pi$ ) interactions among the bent molecules in the liquid.<sup>7</sup>

On the other hand, apart from a large thermal contrast between two or more states, an ideal thermal switch must transform among them as fast as possible upon application

of an external stimulus. In this case, although the crystal-to-liquid transition occurs within few minutes, the full recovery of the original thermal conductivity takes more than an hour. This is due to the low mobility of the large molecules at room temperature, which must diffuse through the liquid and reorganize to form back the *trans* crystal. This process is even more difficult in the case of molecules with longer alkyl chains. The recovery of the higher  $\kappa$  phase can be accelerated by reducing the length of the alkyl chains, and above all, by cycling between the higher mobility *trans*-N-LC and the *cis*-IL (Fig. 3b and c).

The speed of the process is shown in more detail for the different phases in Fig. 4 (see also Fig. S10, ESI†).

Following these results, we hypothesized that the 4,4'-dialkyloxy-3-methylazobenzenes could be used as molecular machines to control the spatial arrangement of an achiral LC matrix, and hence its thermal conductivity. Doping a LC network with light-sensitive molecules has been used previously by several groups to induce macroscopic displacements, through cooperative bending, and transitional, and rotary motions of the molecules of the LC,<sup>17–20</sup> but this approach has never been applied to control the thermal conductivity of a mesophase.

To probe the viability of this hypothesis, we first searched for a system with a large thermal contrast between the LC mesophase and the IL, which is also chemically and structurally compatible with the 4,4'-dialkyloxy-3-methylazobenzenes synthesized in this work.

We identified 4-octyl-4'-cyanobiphenyl (8CB) as a suitable candidate for this study.<sup>21</sup> DSC analysis shows that 8CB presents a smectic mesophase (Sm-LC) at room temperature, which is transformed into N-LC at  $\approx 306 \text{ K}$ , and then to an IL at 314 K (see the ESI† for a complete characterization of the pure 8CB and 8CB:azobenzene mixture; Fig. S13–S18, ESI†).<sup>22</sup> Our thermal conductivity experiments confirmed a reduction of  $\approx 15\text{--}20\%$  between the Sm-LC and IL phases; the N-LC phase of 8CB also shows a lower thermal conductivity than its IL (Fig. S14, ESI†). These results are in very good agreement with Marinelli *et al.*<sup>15</sup>, and confirm the planar orientation of the

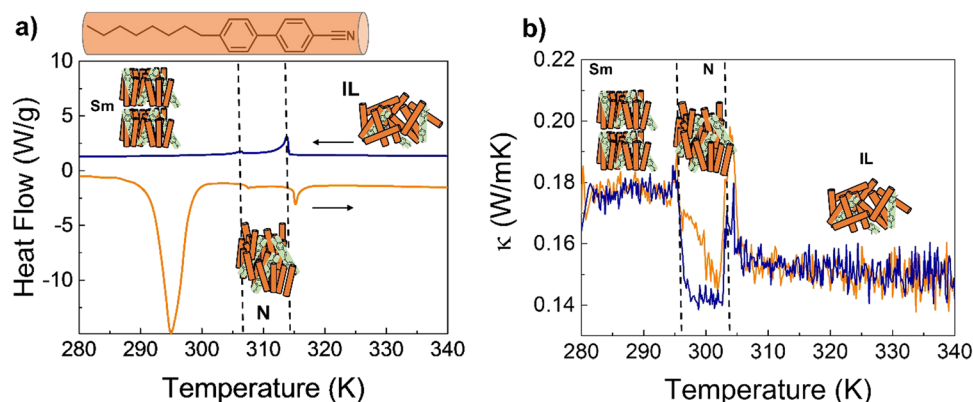
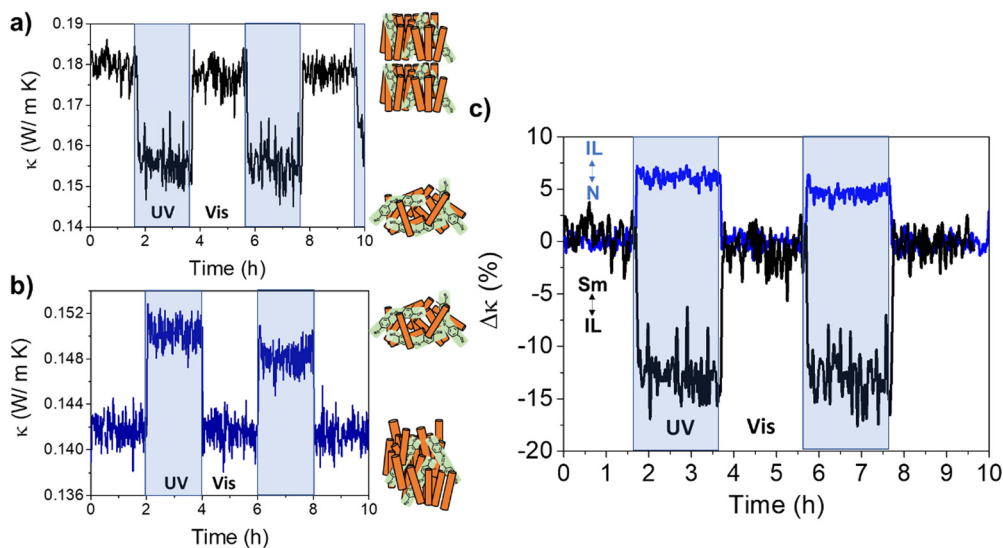


Fig. 5 (a) DSC heating and cooling scans of 8CB:azobenzene dispersion, identifying the thermal stability of the smectic, and nematic phases. (b) Temperature dependence (heating and cooling runs) of the thermal conductivity of 8CB:azobenzene, demonstrating the thermal contrast between the different phases observed in the DSC scan. The differences in the actual temperature of the transition temperatures measured by DSC and thermal conductivity are due to the different scan rates ( $10 \text{ K min}^{-1}$  in DSC and  $1 \text{ K min}^{-1}$  in thermal conductivity).





**Fig. 6** Room temperature light-triggered thermal conductivity switching of 8CB:azobenzene molecular system. Irradiating the Sm phase ( $\approx 290$  K) with UV light, transforms the system to the IL, reducing its thermal conductivity (a). On the other hand, irradiation of the N phase ( $\approx 300$  K) with UV light, transforms the system to the IL and increases its thermal conductivity (b), in perfect agreement with the results in Fig. 5. (c) Bi-directional switching of the thermal conductivity is demonstrated in this figure: either an increase or a decrease of the thermal conductivity can be achieved upon UV illumination of a partially ordered mesophase of 8CB:azobenzene system. Both changes are reversible after illumination with visible light.

LC (director perpendicular to heat flow). Also, the similar values of the heat capacity and sound velocity reported for the different phases of 8CB<sup>15,23</sup> suggest that the lower  $\kappa$  in the N-phase is related to shorter lifetime of vibrational coupling modes across the planar order.

8CB was doped with 4% w/w of the  $n = 6$  4,4'-dialkoxy-3-methylazobenzene; the DSC and  $\kappa(T)$  analysis showed that this level of doping does not affect the transition temperatures or stability of the mesophases of pure 8CB (Fig. 5).

The 8CB:azobenzene Sm-LC was irradiated at 290 K with UV light while measuring the thermal conductivity. The results, shown in Fig. 6(a), demonstrate a reduction of  $\approx 15\%$  consistent with a transition between Sm-LC and IL. This confirms that isomerization of the azobenzene into the *cis* state, induces a cooperative molecular motion which destabilizes the entire bulk Sm-LC mesophase of 8CB.

Irradiating the system at 300 K, within the N-LC stability region, this phase transforms into the IL, resulting in an increase of the thermal conductivity of  $\approx 5\%$ , Fig. 6(b) (see also Fig. S16 and S17, ESI<sup>†</sup>).

The results presented in Fig. 6 show that fast and reversible bi-directional switching of the thermal conductivity may be achieved in achiral LC hosts doped with the adequate photo-responsive molecules.

Finally, as shown in Fig. 7, three different thermal states can be accessed in UV/dark irradiation cycles in 8CB:azobenzene: after UV illumination ceases, azobenzene molecules in the IL recover their *trans* rod-like structure in the dark, and the whole system relaxes into the Sm-LC through an intermediate phase of lower thermal conductivity. POM images (Fig. S18, ESI<sup>†</sup>) also show the rapid transition to this intermediate phase in the dark, before relaxing slowly to the Sm-LC.

Although the intermediate phase cannot be univocally identified from POM, it does show the same thermal conductivity as the N-phase in Fig. 5(b). Therefore, the most plausible situation is that the system relaxes in the dark very fast from IL-to-N, and slowly adopts the more ordered Sm-LC phase.

Given the different thermal conductivities between the three phases, three different thermal states can be achieved in a *single* UV/dark run in this composite molecular system.

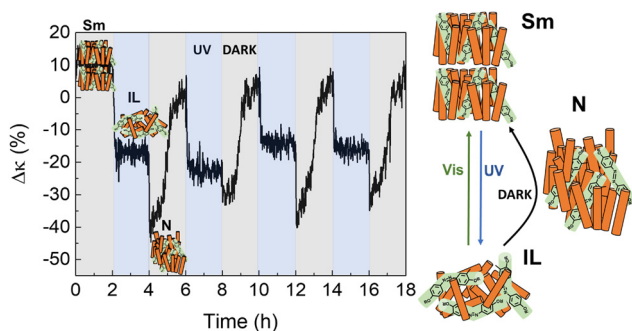


**Fig. 7** UV/Dark cycles of 8CB: azobenzene molecular system at  $\approx 290$  K. Three different thermal states can be identified in this case, associated with the different  $\kappa$  values of the Sm-LC, N-LC and IL, as observed in Fig. 5(b).

## Conclusions

Pure 4,4'-dialkoxy-3-methylazobenzene molecular materials can be switched between higher/lower thermal conductivity states under mild UV/Vis irradiation conditions around room temperature.



These photochromic molecules may act as light-driven molecular machines which reversibly operate over the bulk order of conventional LC mesophases, allowing reversible access to more than two thermal states and bi-directional switching of their thermal conductivity. Larger thermal contrasts may be observed in homeotropically aligned LC.

The variety of available LC, with different mesophases which could be accessed through doping with chemically compatible photoactive molecules, might open a new area of research for the design of molecular materials with multiple, accessible, thermal states around room temperature.

## Methods

4,4'-Dialkoxo-3-methylazobenzene derivatives were synthesized following a modification of a previously described route<sup>11</sup> (see the ESI† for a detailed description of the synthetic procedure). 4-Octyl-4'-cyanobiphenyl (8CB), was purchased from Sigma-Aldrich and used without further purification.

Structural characterization of these compounds was performed by <sup>1</sup>H-NMR using Bruker Advance DRX-500 and Varian Mercury-300 spectrometers. The recorded spectra are in agreement with the literature data.<sup>11,12</sup>

Polarized optical microscopy (POM) images were taken using a Leica DM2700 M microscope, equipped with a Linkam stage and a LNP96-S liquid nitrogen pump that allow precise control of temperature. UV-Vis absorption spectra were recorded on a Jasco V-630 spectrophotometer, coupled with a Jasco ETC-717 temperature controller. DSC measurements were carried out using a TA Instruments Q200 calorimeter. Thermal conductivity measurements were performed in a liquid nitrogen cryostat using a 3 $\omega$  method, with a home-made setup as described in ref. 13. Further details of all the procedures are provided in the supporting information accompanying this paper.

## Data availability

All data, and materials used in the analyses are available, upon reasonable request.

## Conflicts of interest

There are no conflicts to declare.

## Acknowledgements

We acknowledge a fruitful discussion of the results and the manuscript with Dr Jonathan Malen (Carnegie Mellon University, USA) and Dr Nikos Doltsinis (University of Münster, Germany). This work has received financial support from Ministerio de Economía y Competitividad (Spain): projects PID2019-104150RB-I00 and RTI2018-101097-A-I00; Xunta de Galicia (Centro singular de investigación de Galicia acreditación 2019-2022, ED431G 2019/03 and ED431B 2021/13); the

European Union (European Regional Development Fund-ERDF and European Research Council (ERC) Starting Investigator Grant (NANOCOMP-679124)). N. V. D. acknowledges financial support from Fundación Segundo Gil Dávila and MINECO (Spain) through an FPI fellowship (PRE2020-096467). A.L.M. and M.G-L. thank Agencia Estatal de Investigación for financial support (Juan de la Cierva de Formación fellowship (FJC2018-037044) and Ramon and Cajal contract (RYC-2016-20258)). A.L.M., G.R. V.L. and N. V. D. were also supported by the project ERC-StG-679124.

## References

- 1 E. Langenberg, D. Saha, M. E. Holtz, J. J. Wang, D. Bugallo, E. Ferreira-Vila, H. Paik, I. Hanke, S. Ganschow, D. A. Muller, L. Q. Chen, G. Catalan, N. Domingo, J. Malen, D. G. Schlom and F. Rivadulla, Ferroelectric Domain Walls in PbTiO<sub>3</sub> Are Effective Regulators of Heat Flow at Room Temperature, *Nano Lett.*, 2019, **19**, 7901–7907.
- 2 J. J. Wang, Y. Wang, J. F. Ihlefeld, P. E. Hopkins and L. Q. Chen, Tunable thermal conductivity via domain structure engineering in ferroelectric thin films: A phase-field simulation, *Acta Mater.*, 2016, **111**, 220–231.
- 3 B. M. Foley, M. Wallace, J. T. Gaskins, E. A. Paisley, R. L. Johnson-Wilke, J. W. Kim, P. J. Ryan, S. Trolier-Mckinstry, P. E. Hopkins and J. F. Ihlefeld, Voltage-Controlled Bistable Thermal Conductivity in Suspended Ferroelectric Thin-Film Membranes, *ACS Appl. Mater. Interfaces*, 2018, **10**, 25493–25501.
- 4 T. Ishibe, T. Kaneko, Y. Uematsu, H. Sato-Akaba, M. Komura, T. Iyoda and Y. Nakamura, Tunable Thermal Switch via Order-Order Transition in Liquid Crystalline Block Copolymer, *Nano Lett.*, 2022, **22**, 6105–6111.
- 5 J. A. Tomko, A. Pena-Francesch, H. Jung, M. Tyagi, B. D. Allen, M. C. Demirel and P. E. Hopkins, Tunable thermal transport and reversible thermal conductivity switching in topologically networked bio-inspired materials, *Nat. Nanotechnol.*, 2018, **13**, 959–964.
- 6 J. Shin, J. Sung, M. Kang, X. Xie, B. Lee, K. Min and T. J. White, Light-triggered thermal conductivity switching in azobenzene polymers, *Proc. Natl. Acad. Sci. U. S. A.*, 2019, 2–7.
- 7 X. Wei and T. Luo, Effect of side-chain  $\pi$ - $\pi$  stacking on the thermal conductivity switching in azobenzene polymers: a molecular dynamics simulation study, *Phys. Chem. Chem. Phys.*, 2022, **24**, 10272–10279.
- 8 T. Ikeda and O. Tsutsumi, Optical Switching and Image Storage by Means of Azobenzene Liquid-Crystal Films, *Science*, 1995, **268**, 1873–1875.
- 9 S. Sun, S. Liang, W.-C. Xu, G. Xu and S. Wu, Photoresponsive polymers with multi-azobenzene groups, *Polym. Chem.*, 2019, **10**, 4389.
- 10 T. van Leeuwen, A. S. Lubbe, P. Štacko, S. J. Wezenberg and B. L. Feringa, Dynamic control of function by light-driven molecular motors, *Nat. Rev. Chem.*, 2017, **1**, 0096.



- 11 Y. Norikane, E. Uchida, S. Tanaka, K. Fujiwara, E. Koyama, R. Azumi, H. Akiyama, H. Kihara and M. Yoshida, Photo-induced Crystal-to-Liquid Phase Transitions of Azobenzene Derivatives and Their Application in Photolithography Processes through a Solid-Liquid Patterning, *Org. Lett.*, 2014, **16**, 5012–5015.
- 12 Y. Norikane, E. Uchida, S. Tanaka, K. Fujiwara, H. Nagai and H. Akiyama, Photoinduced Phase Transitions in Rod-shaped Azobenzene with Different Alkyl Chain Length, *J. Photopolym. Sci. Technol.*, 2016, **29**, 149–157.
- 13 C. López-Bueno, D. Bugallo, V. Leborán and F. Rivadulla, Sub- $\mu$ L measurements of the thermal conductivity and heat capacity of liquids, *Phys. Chem. Chem. Phys.*, 2018, **20**, 7277–7281.
- 14 X. Wei, Z. Wang, Z. Tian and T. Luo, Thermal Transport in Polymers: A Review, *J. Heat Transfer*, 2021, **143**, 072101.
- 15 M. Marinelli, F. Mercuri, S. Foglietta, U. Zammit and F. Scudieri, Anisotropic heat transport in the octylcyanobiphenyl (8CB) liquid crystal, *Phys. Rev. E*, 1996, **54**, 1604.
- 16 G. Ahlers, D. S. Cannell, L. I. Berge and S. Sakurai, Thermal conductivity of the nematic liquid crystal 4-*n*-pentyl-4'-cyanobiphenyl, *Phys. Rev. E*, 1994, **49**, 545.
- 17 B. L. Feringa, In control of motion: from molecular switches to molecular motors, *Acc. Chem. Res.*, 2001, **34**, 504–513.
- 18 D. R. S. Pooler, A. S. Lubbe, S. Crespi and B. L. Feringa, Designing light-driven rotary molecular motors, *Chem. Sci.*, 2021, **12**, 14964–14986.
- 19 R. Eelkema, M. M. Pollard, J. Vicario, N. Katsonis, B. S. Ramon, C. W. M. Bastiaansen, D. J. Broer and B. L. Feringa, Nanomotor rotates microscale objects, *Nature*, 2006, **440**, 163.
- 20 J. Hou, G. Long, W. Zhao, G. Zhou, D. Liu, D. J. Broer, B. L. Feringa and J. Chen, Phototriggered Complex Motion by Programmable Construction of Light-Driven Molecular Motors in Liquid Crystal Networks, *J. Am. Chem. Soc.*, 2022, **144**, 6851–6860.
- 21 C. Fehr, P. Dieudonné, J. Primera, T. Woignier, J.-L. Sauvajol and E. Anglaret, Solid state polymorphism of liquid crystals in confined geometries, *Eur. Phys. J. E: Soft Matter Biol. Phys.*, 2003, **12**, 13–16.
- 22 J. Thoen, H. Marynissen and W. Van Dael, Temperature dependence of the enthalpy and the heat capacity of the liquid-crystal octylcyanobiphenyl (SOB), *Phys. Rev. A: At., Mol., Opt. Phys.*, 1982, **26**, 2886–2905.
- 23 I. Chaban, C. Klieber, R. Busselez, K. A. Nelson and T. Pezeril, Crystalline-like ordering of 8CB liquid crystals revealed by time-domain Brillouin scattering, *J. Chem. Phys.*, 2020, **152**, 014202.

